Chapter 76

Development of Hybrid Linear Friction Welding of overlap and T joints in aluminum alloys

Ricardo Maciel
LAETA, IDMEC, Instituto Superior Técnico, Universidade de Lisboa, Av. Rovisco Pais, 1, Lisboa, 1049-001, Portugal

Daniel F.O. Braga
LAETA, IDMEC, Instituto Superior Técnico, Universidade de Lisboa, Av. Rovisco Pais, 1, Lisboa, 1049-001, Portugal

Virgínia I. M. N. Infante
LAETA, IDMEC, Instituto Superior Técnico, Universidade de Lisboa, Av. Rovisco Pais, 1, Lisboa, 1049-001, Portugal

Pedro M.G.P. Moreira
INEGI, Universidade do Porto, Rua Dr. Roberto Frias, 400, Porto, 4200-465, Portugal

Lucas F.M. da Silva
FEUP, Universidade do Porto, Rua Dr. Roberto Frias, s/n, Porto, 4200-465, Portugal

ABSTRACT
While Linear Friction Welding (FSW) has been shown to produce high performance butt joints, stress concentration at the weld edges in the FSW lap significantly reduces the performance of these joints. In this article, the research studies carried out will be presented, referring to the development of the process of joining metals, linear friction welding (FSW) in combination with adhesive bonding (AB), Friction Stir Weld-Bonding (FSWB), for overlapping joints (SLJ) and AA 6082-T6 aluminum alloy T-joints. Before the manufacturing of optimized joints was achieved, it was necessary to carry out several experimental weldings to select the FSW parameters for the lap and T joints. The current article intends to present the results obtained for the different tests carried out, as well as the discussion of these, regarding the improvement of the fatigue strength of lap joints using the FSWB process when compared to the FSW process. FSWB welding achieved a significant increase in quasi-static and fatigue strength when compared to FSW overlay, with 79.9% of the adhesive joint fatigue strength at 106 cycles, while FSW had 41.6%. bending of T-joints in an integral frame configuration will also be presented and discussed.

Keywords: Linear Friction Welding (FSW); Adhesive Bonding (AB); Aluminum Alloy; Fatigue; Hybrid Linear Friction (FSWB).
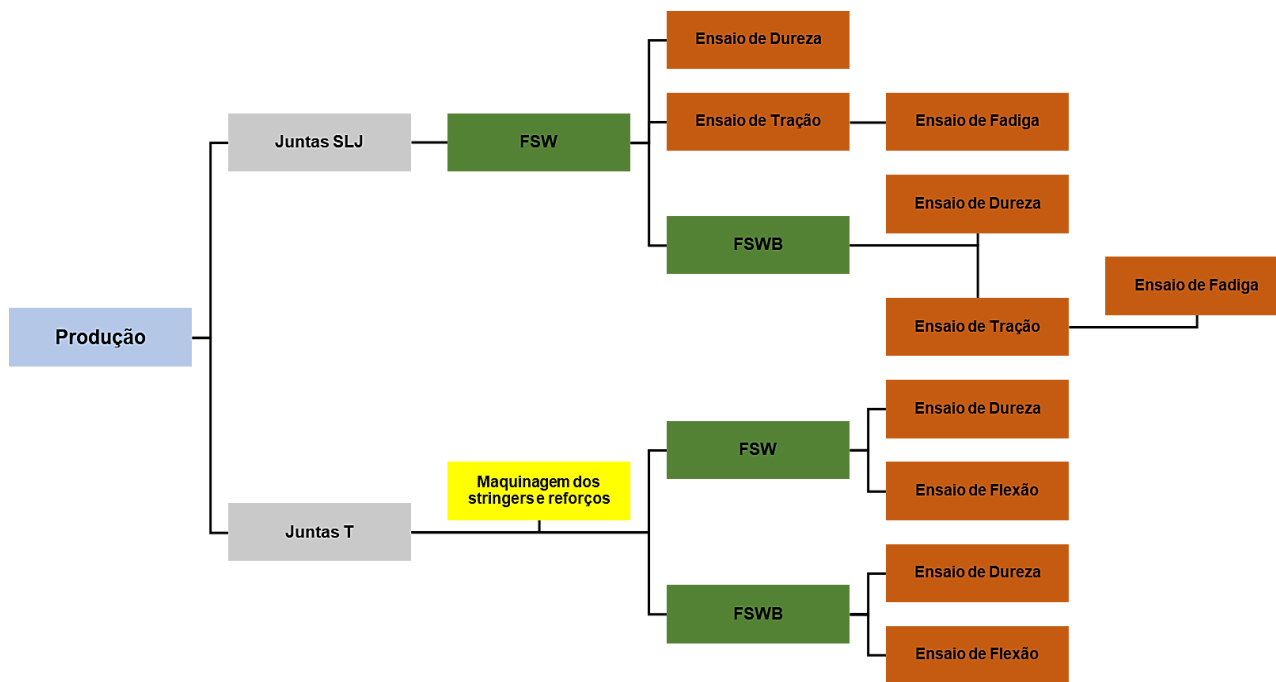
1 INTRODUCTION

The combination of new regulatory requirements [1] and market demand [2], [3] push for continuous improvements in energy efficiency and performance of transport solutions. Weight reduction can be accomplished through the use of new light alloys and new structural designs [3]. To implement the use of lighter materials and innovative structural designs, it is necessary to develop new manufacturing processes.

For decades, aircraft structures have been joined using a variety of joining techniques, including welding. The aeronautical industry makes little use of welding processes in primary structures due to the loss of mechanical properties related to large heat inputs, welding quality control (process reliability) and the impossibility of welding precipitation-hardened alloys (for example , AA2024 aluminum alloy), in

which cracks tend to form from welds involving melting of the material. In the last 15-20 years, there have been significant developments in binding techniques [4]. In this article, a hybrid bond is presented, a combination of friction welding processes, FSW (Friction Stir Welding), and adhesive bonding, AB (Adhesive Bonding). The development of this new hybrid bonding technology, Friction Stir Weld-Bonding (FSWB), aims to incorporate properties and characteristics of both bonding technologies, as well as to improve damage tolerance.

Figure 1 shows the developed experimental work program. The manufacture of lap joints (SLJ) by the FSW process was the first step. The FSWB lap joints were manufactured after an evaluation of the parameter sets used in FSW welding. The different types of produced joints were evaluated and compared, according to the quasi-static and fatigue behavior. Finally, the T-joints were manufactured, requiring a new evaluation of the welding parameters in the laboratory, due to the complex geometry of the joint. The geometry of the T-joint is made up of four parts, and three of these parts need to be machined before welding.

Figure 1: Work program

SUBTITLE: Production   attraction test
SLJ gaskets   FSWB
T joints   FSW
FSW   FSWB
Machining of stringers reinforcements   fatigue test
hardness test

2 MANUFACTURE OF OVERLAPPED JOINTS (SLJ)

2.1 BASE MATERIAL CHARACTERIZATION

When compared with 6000 series, AA6082 aluminum alloy has a high strength, which can be increased by solubilization heat treatment and artificial aging, T6. As part of the 6000 series alloys, the

main components are magnesium and silicon that precipitate in the form of Mg2Si (β phase) within the aluminum matrix of the α phase [5]. Alloy AA 6082-T6 contains manganese to increase ductility and strength. The chemical composition and mechanical properties of the AA6082-T6 alloy are presented in Tables 1 and 2

Table 1: Chemical composition of AA6082-T6(% mass) [6]

Man-ganese (Mn)	Iron (Fe)	Mag-nesium (Mg)	Silicon (Si)	Coper (Cu)	Zinc (Zn)	Tita-nium (Ti)	Choro-mium (Cr)	Others (Total)	Alu-minium (Al)
0.40 1.00	0.50	0.60 1.20	0.70 1.30	0.10	0.20	0.10	0.25	0.10	Balance

Tabela 2: AA6082-T6 mechanical properties [6]

Density (kg/m³)	Vickers Hardness	Ultimate Tensile Strength (MPa)	Yield Tensile Strength (MPa)	Elongation at Break (%)
2700	95	290	250	10

He used the DIC (Digital Image Correlation) measurements in the tensile tests of 3 mm thick welds, in order to obtain stress-strain curves of the different regions identified in the weld. Butt joints were produced by the FSW process in AA6082-T6 aluminum alloys.

Figure 2: Actual stress vs. actual strain curves for different sections of material.
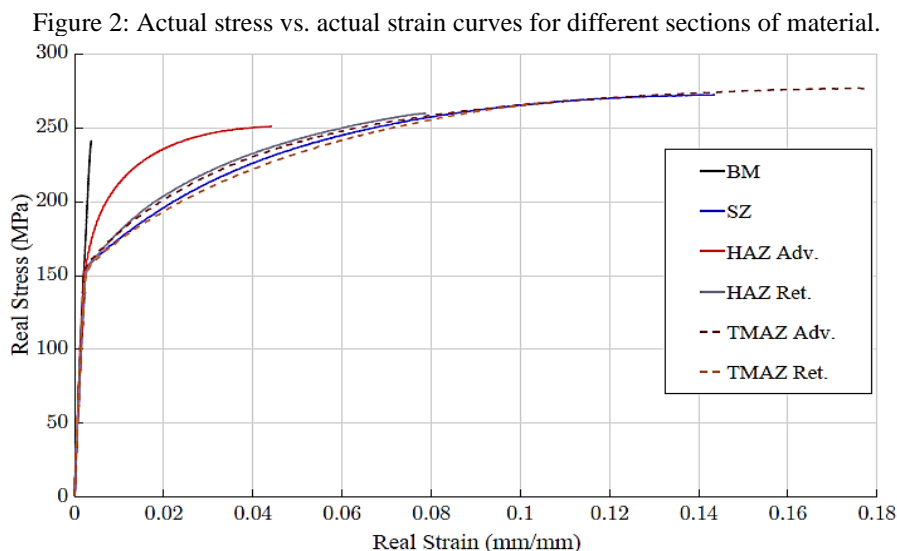
3 STICKER CHARACTERIZATION

The adhesive applied to the joints was Huntsman® Araldite 420 A/B, a two component epoxy adhesive. The two components must be mixed with a nozzle mixer and the mixture must have a dark green color, as per Table 3.

Table 3: Typical data for adhesive 420 A/B [7]

Property	Araldite 420 A	Araldite 420 B	Mixed adhesive	Test Method
Colour (visual)	yellow	blue	dark green	visual
Specific gravity	ca.1.2	ca.1.0	1.1 - 1.2	ASTM-D-792
Viscosity at 25°C (Pas)	100 - 300	0.6 - 1.4	35 - 45	ASTM-D-2196
Gel time (100 gm at 25°C) mins	-	-	60	ASTM-D-2471

During FSW welding of hybrid joints (FSWB), the uncured adhesive will be subjected to an elevated temperature which can locally accelerate the curing process. Differential Scanning Calorimetry (DSC) was used to evaluate the healing process of the chosen adhesive. DSC analysis was performed on a Netzsch® DSC 200 F3 instrument on samples with a mass of ≈50 mg, at a constant heating rate of (20 K)/min from 21°C to 320°C in a constant flow atmosphere of 20 mL⁄min of N2.

To evaluate the mechanical properties of the adhesive, the method used was the tensile test on specimens of solid adhesive, Bulk Tensile, carried out at a transverse speed of 1 mm / min in an Instron testing machine. Tensile tests on bulk specimens were performed under 4 different curing conditions: (i) room temperature for 7 days; (ii) 120°C for 1 hour as indicated on the adhesive data sheet; (iii) 165°C for 30 minutes and (iv) 200°C for 30 minutes. An increase in maximum resistance was observed with increasing temperature [8].

Thermogravimetric analysis (TGA) of the uncured adhesive was performed and TG (Glass Transition Temperature) curves were obtained, where the onset of significant degradation was found at $⟦357⟧_{(-3)}^{(+2)}$ °C [8].

Given the complexity of loading on overlapping joints [9] , the fracture toughness of the adhesive in modes I and II was evaluated using Double Cantilever Beam (DCB) specimens and End Notched Flexure (ENF) specimens, respectively. The DCB test was performed at a transverse velocity of 1 mm/min and the curves obtained were used to draw the corresponding R curves using the Compliance-Based Beam Method (CBBM). The energy release rate in mode I was 3±0.37 N/mm [8]. For mode II, the ENF test was performed at a transverse velocity of 0.2 mm/min and analyzed by the CBBM method. The obtained value of 9 N/mm, for critical fracture toughness in mode I, resulted in better agreement with the curves [8].

Table 4 summarizes the mechanical properties for two curing temperatures.

Table 4: Mechanical properties of Araldite 420 A/B adhesive.

| Cure condition	E (GPa)	G (MPa)	σ (MPa)	τ (MPa)	G_I^c (N/mm)	G_{II}^c (N/mm)
Room Temperature for 7+ days	1.57	600	30	22.5	3	9[+]
120°C for 1 h	1.73	665	40	28	3[*]	9[+,*]

4 SURFACE TREATMENT

The treatment applied to the surfaces to be bonded in the FSWB welded joints was Sol-Gel, developed by the Boeing Company. The product applied is 3MTM AC-130, which has been normally used in aircraft repair [10]. This product promotes adhesion by forming a surface oxide layer. This treatment is faster than conventional phosphoric acid (PAA) anodizing and results in similar bond strength. In addition, it is easier to perform in relatively large areas, as is the case with FSWB welded joints, as it requires less laboratory equipment.

4.1 JOINT GEOMETRY

The FSW and FSWB joints were manufactured with an overlap of 40 mm and 20 mm and with an adhesive thickness of 0.2 mm, as shown in Figure 3. The thickness of the adhesive was guaranteed with calibrated steel tapes. An overlap width of 40 mm is significantly smaller than current fixed joint designs for aeronautical fuselages [11], such as longitudinal fuselage joints, leading to weight savings. To keep the bending moment constant in both configurations, the following dimensions were used: (i) 300 x 130 x 2 mm for the 20 mm overlapping joints and (ii) 300 x 150 x 2 mm for the 20 mm overlapping joints 40 mm. For adhesive joints, each adherent was 25 x 150 x 2 mm. All sheets were cut so that the rolling direction was aligned with that of the weld.

Figure 3: Cross-section of overlap joints: a) 20 mm overlap and b) 40 mm overlap.
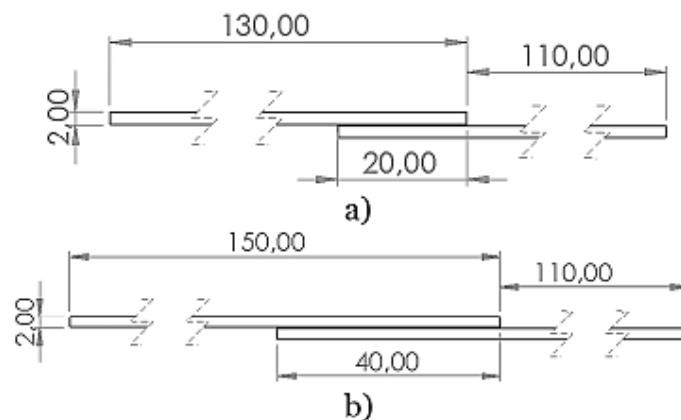
4.2 TOOLING FSW

A patented modular concept of the FSW tool comprising three main components; body, shoulder and pin was used to produce the joints in this investigation. A threaded cylindrical pin with a diameter of 5 mm was mounted on a flat shoulder with spirals and a diameter of 16 mm, as shown in Figure 4. The length of the pin was adjusted to approximately 3 mm, in order to promote an ideal mixing in the zone of agitation.

Figure 4: FSW tooling

5 PROCEDIMENTO EXPERIMENTAL

Linear friction welds (FSW) were produced on a dedicated LEGIO 3UL numerical control machine from ESAB® (Gothenburg, Sweden) (Figure 5). This machine is capable of welding in both position control and force control. When inserted into the machine, the tool has three degrees of freedom: x, y and z. The protection of the integrity of the tool, during the welding process, is carried out by a water cooling system, available in the machine.

Figure 5: FSW LEGIO 3UL - ESAB® machine

When discussing welding methods and adhesive bonding, weld-bonding, hybrid joints, there are two distinct methodologies, "flow-in" and "weld-through". Figure 6 illustrates the two mentioned manufacturing methods. The weld-through method is the most used, first the adhesive paste is applied to one of the sheets, followed by the welding procedure. Then the adhesive is cured [12].

Table 5: FSW process parameters

Parâmetros	Valores
Controlo FSW	Força Vertical
Direção de Rotação	CW
Velocidade de Penetração	0,1 mm/s
Dwell Time	6 s
Ângulo de Inclinação	0°
Velocidade de avanço	200 mm/min
Velocidade de rotação	1000 rpm
Força axial	400/425/450/500/550 kgf

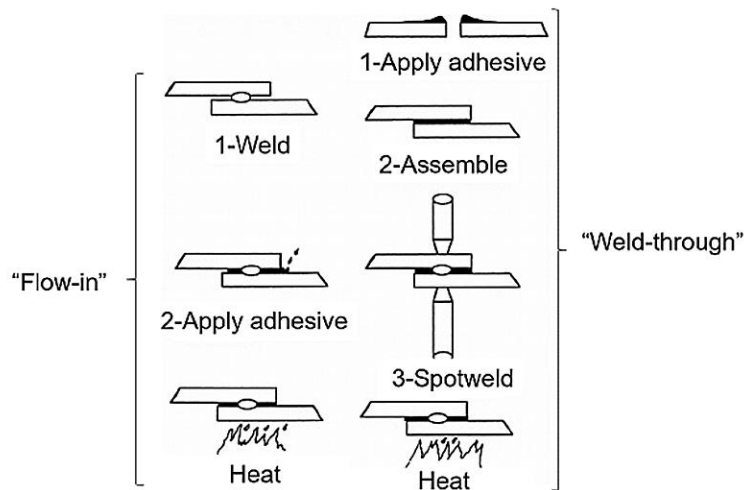Figure 6: Manufacturing process used in weld-bonding [12].

Table 6 lists all FSW and FSWB lap joints produced and the parameter combinations studied in this investigation.

Table 6: Produced lap joints.

| Designação da junta	Força Axial [kgf]	Sobreposição [mm]
FSW 400 -1	400	40
FSW 425 -1	425	20
FSW 450 - 1	450	40
FSW 500 - 1	500	40
FSW 550 - 1	550	40
FSW+AB 400 - 1	400	40
FSW+AB 400 - 2	400	40
FSW+AB 425 - 1	425	20
FSW+AB 425 - 2	425	40
FSW+AB 450 - 1	450	40
FSW+AB 450 - 2	450	40
FSW+AB 450 - 3	450	40
FSW+AB 500 - 1	500	40
FSW+AB 550 - 1	550	40

After the welding process, the joints produced were cut into 25 mm wide specimens, in accordance with ASTM D1002 [13], as shown in Figure 7.

Figure 7: Specimens cut according to ASTM D1002 standard.
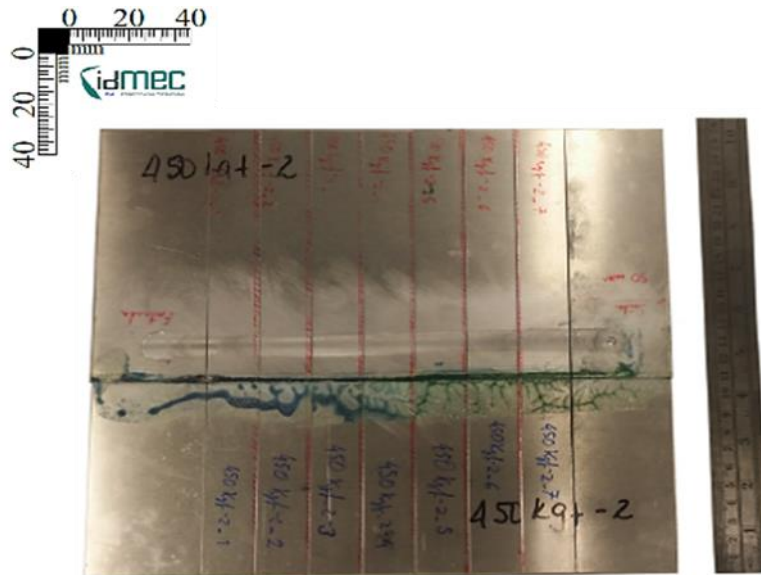
The metallographic characterization of welded joints is a common destructive procedure in friction welding, in order to analyze the welded region and verify whether the weld parameters induce internal defects [14].

Figure 8: General macrostructure of the AA6082-T6 hybrid lap joints.
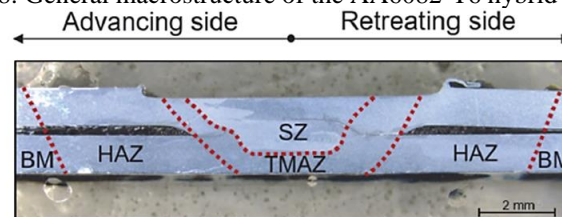

5.1 MECHANICAL CHARACTERIZATION

The mechanical characterization is mainly composed of tensile strength tests, fatigue strength and microhardness measurements in the cross-section of the weld.

Microhardness measurement

The samples were also subjected to a microhardness measurement. Measurements were performed on a Digital Microhardness Tester HMV-2 (Micro Hardness Tester), applying a load of 0.2 HV (1.961 N) for 10 seconds in each indentation. The samples used were taken from joints labeled "FSW+AB-450-1" and "FSW+AB-400-1", Table 6. The results are shown in Figures 9 and Figure 10.

Figure 9: Microhardness values of the cross-section of the "FSW+AB-450-1" sample.
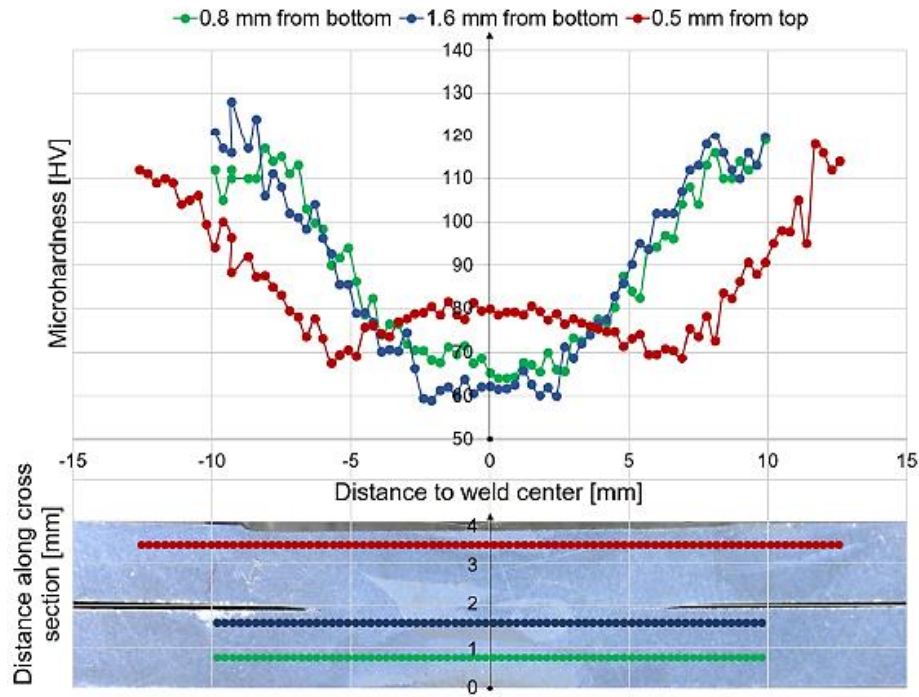
In the welding region, Figure 9, softening is observed around the agitation zone (WN), as reported in the literature [15]. The lowest hardness value is located far from the center line, at the WN limits, about 5 mm for the upper measurements, in red, and 2.5 mm for the lower ones, blue and green, which is equivalent to the limits of the dimension of the pin. In this region of minimum hardness, only low-density rod-shaped precipitates are present, which causes a reduction in hardness [16].

From Figure 10, it is possible to conclude that the different axial forces applied by the tool have very little influence on the microhardness distribution.

Figure 10: Microhardness values of the 400 kgf and 450 kgf samples.
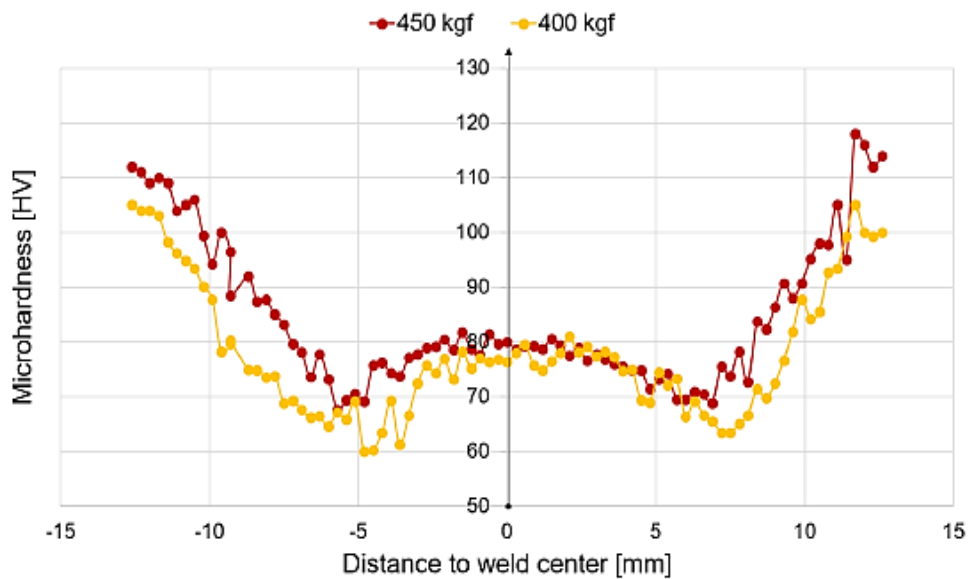
Traction Tests

In order to determine the tensile mechanical properties of welds in the FSW and FSWB process, such as yield strength σ_0, breaking stress σ_u, breaking length ε_u and Young's modulus E, shear strength tests were carried out on specimens cut with 2 mm thick, as per ASTM D1002. Shims were used to avoid the formation of a bending moment that would distort the results.

The tests were carried out using an INSTRON R 3369 universal testing machine with a maximum load capacity of 50 kN. The transverse velocity was 1 mm/min. The stress in the joint was calculated considering the remote section of the joint, as shown in Figure 11.

Figure 11: Area considered for stress calculation in the joint [17]
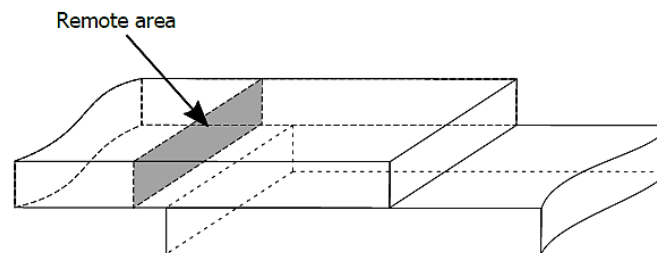
In the tensile tests of the FSW and FSWB lap joints, the load was applied on the advancing side, and fracture occurred in two failure modes:

- In the first fracture mode, mode I, Figure 12, the fracture starts on the weld setback side, starting in the cold lap type defect and propagating parallel to the upper surface in the direction of the hook type defect [18].

Figure 12: Different views of the first fracture mode.

- In the second fracture mode, mode II, Figure 13, the fracture occurred on the welding advance side, starting at the hook defect and then propagating perpendicularly to the upper surface [19]. In mode II, the force creates a sliding or shearing mode perpendicular to the leading edge of the crack.

Figure 13: Different views of the second fracture mode.
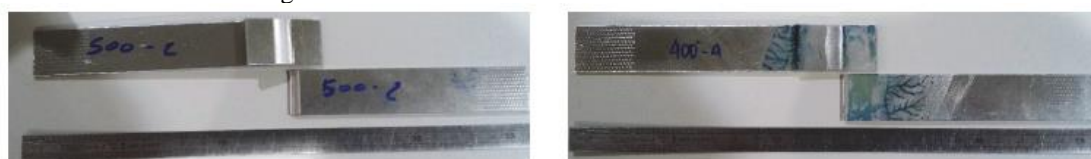
Mean maximum load values were calculated for all different configurations, Table 7 - FSW and Table 8 - FSWB, to estimate the maximum ultimate stress, σ_u. In addition, ductility was obtained by measuring the maximum displacement in each case.

Table 7: Results of shear resistance tests for FSW joints.

Joint tag	Average maximum load [kN]	Maximum load dispersion [kN]	Average maximum displacement [mm]	Maximum displacement dispersion [mm]	σ_u [MPa]
FSW-400 - 1	7.21	0.10	1.88	0.02	144.2
FSW-450 - 1	7.61	0.12	2.00	0.21	152.2
FSW-500 - 1	8.84	0.16	2.35	0.17	176.8
FSW-550 - 1	9.10	0.80	2.47	0.41	188.2

Table 8: Characteristics of the shear resistance tests of FSWB joints.

Joint tag	Average maximum load [kN]	Maximum load dispersion [kN]	Average maximum displacement [mm]	Maximum displacement dispersion [mm]	σ_u [MPa]
FSW+AB-400 - 1	10.63	3.66	2.10	0.76	212.6
FSW+AB-450 - 1	12.22	2.40	3.15	1.14	244.4
FSW+AB-500 - 1	11.64	2.28	2.66	0.47	232.8
FSW+AB-550 - 1	11.15	1.23	1.99	0.21	223.0

By comparing the rupture stress of the joints produced with the base material, it is possible to obtain the efficiency of the joint. A specimen with the base material, AA6082-T6, and the same dimensions as the welded specimens, was tested and $\sigma\_u= 331.4$ MPa was obtained. Figure 14 presents the calculated joint efficiency, for each type of joint according to the applied axial force, including the dispersion of the results.

Figure 14: Efficiency values of FSW and FSWB joints.

The FSWB joints present better overall results and, as previously mentioned, the best efficiency achieved was in the joint produced with 450 kgf. The average efficiency value in this case was 73.75%, however, in one of the samples, it reached a value of 85.21%. From the results, Figure 14, it is possible to state that the hybridization process provides an improvement in mechanical performance between 20 and 30% in most cases.

Fatigue Tests

Joint and specimen configurations tested under quasi-static shear tensile load were tested under cyclic tensile conditions to evaluate and compare their fatigue strengths. Thus, the FSW and FSWB specimens were submitted to a cyclic load with a stress ratio R=σ_min/σ_max of 0.1, together with the

adhesive joints. The stopping criterion was set at 2 x 10⁶ cycles. Four or five stress levels with three specimens each were used to plot the stress versus number of cycles curves. The tests were performed on the INSTRON R 8874 hydraulic servo machine.

To address the probabilistic nature of the fatigue life analysis resulting from experimental dispersion in cyclic loading tests, a probabilistic fatigue model was used [20]. ProFatigue software was used to establish probabilistic stress life curves [21].

The FSWB (FSW+AB) and FSW joints produced with an axial force of 450 kgf and together with the adhesive joints, were subjected to cyclic loading to evaluate the resistance to fatigue. The experimental results obtained in these joints were plotted in an S-N curve, together with the failure probability of 50% and 5%, as shown in Figure 15. Joint and specimen configurations tested under quasi-static shear tensile load were tested under cyclic tensile conditions to evaluate and compare their fatigue strengths. Thus, the FSW and FSWB specimens were submitted to a cyclic load with a stress ratio $R = \sigma\_min / \sigma\_max$ of 0.1, together with the adhesive joints. The stopping criterion was set at 2 x 10⁶ cycles. Four or five stress levels with three specimens each were used to plot the stress versus number of cycles curves. The tests were performed on the INSTRON R 8874 hydraulic servo machine.

To address the probabilistic nature of the fatigue life analysis resulting from experimental dispersion in cyclic loading tests, a probabilistic fatigue model was used [20]. ProFatigue software was used to establish probabilistic stress life curves [21].

The FSWB (FSW+AB) and FSW joints produced with an axial force of 450 kgf and together with the adhesive joints, were subjected to cyclic loading to evaluate the resistance to fatigue. The experimental results obtained in these joints were plotted in an S-N curve, together with the failure probability of 50% and 5%, as shown in Figure 15.

Figure 15: P-S-N curves of the three types of joints: adhesive bonding, FSW and FSWB.
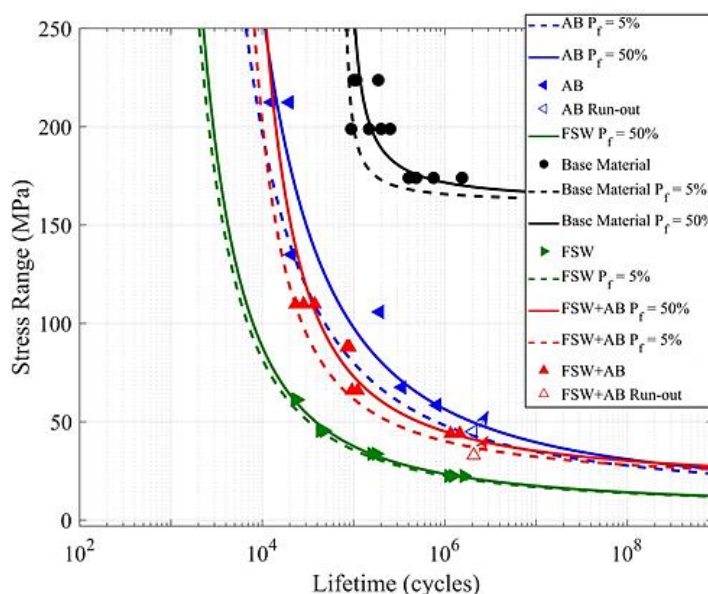
In the fatigue tests, the observed failure modes were similar to those presented in the quasi-static tensile tests, with the samples fracturing on the advancing side for the FSW and FSWB joints.

In the cyclic loading, Figure 15, the adhesive bond reached the highest resistance to fatigue followed by the FSWB welding (79.9% of resistance of the adhesive joints in 106 cycles) and the FSW that presented significantly lower resistance to fatigue (41.6% of strength of adhesive joints at 106 cycles).

6 MANUFACTURE OF T JOINTS

The T-joint is an important type of geometry when it is necessary to significantly increase the inertia and resistance of skins or thin sheets, without a significant increase in weight, which is particularly relevant in transport structures. Aluminum alloy T-joints welded by fusion techniques exhibit large residual stresses and significant distortion due to the high temperatures reached during welding. When compared with melting techniques, the FSW process has a better surface finish, no porosity, no segregation or hot cracking, and no need for consumables [22,23].

In this study, T joints were produced by the FSW and FSWB processes. The FSWB process for T-joints is innovative. The weld-through method was adopted no desenvolvimento da união FSWB.

6.1 JOINT GEOMETRY

The T-joints, FSW and FSWB, were manufactured with a geometry composed of four parts, this configuration, object of patent 109651 PT - INEGI, has reinforcement plates on the advancing and receding sides, which allow the welding combination (FSW), with structural bonding (AB), to form an FS weld-bonding (FSWB) process.

The T joint configuration, Figure 21, has the following dimensions: (i) Skin: 250 x 200 x 2 mm; (ii) Stringer: 250 x 31 x 2 mm and (iii) Reinforcement (2 pieces): 250 x 14 x 2 mm. The adhesive thickness used was 0.2 mm, guaranteed with calibrated steel tapes. The sheets were cut, skin and reinforcement, so that the rolling direction was aligned with the welding direction. The base material used to manufacture the T-joints was aluminum alloy AA6082-T6, and the adhesive was Huntsman® Araldite 420 A/B. These materials were the same used in the manufacture of overlapping joints.

Figure 21: Cross-sectional dimensions of the T-joint geometry in [mm].
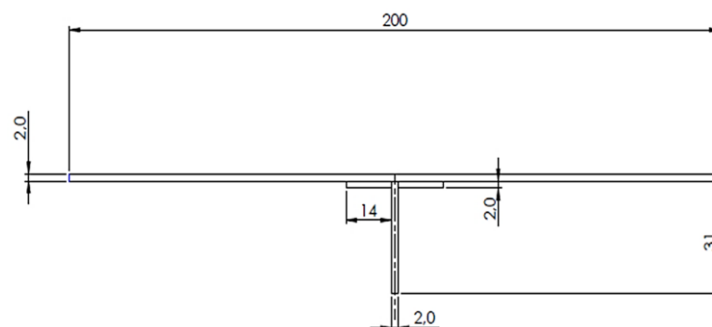
6.2 SURFACE TREATMENT

The treatment applied to the surfaces to be glued in the FSWB welded joints was the process of anodizing in phosphoric acid (PAA), according to ASTM D 3933.

6.3 TOOLING FSW

The FSW tool used to produce the T-joints is composed of a threaded conical pin with a diameter of 7 mm, mounted on a flat shoulder with spirals and a diameter of 18 mm, as shown in Figure 22.

Figure 22: FSW tooling

6.4 EXPERIMENTAL PROCEDURE

Immediately after preparing the surfaces to be bonded to the FSWB joints, the sheets are taken to the numerical control machine LEGIO 3UL by ESAB® (Figure 5) to be welded. The template used to fix the T-joint components to be welded is shown in Figure 22.

Figure 22: a) Fixing system; b) Positioning of the stringer and reinforcements; c) Application of the adhesive; d) Positioning of the skin and fastening system fastened.

Table 9 presents the welding parameters used in the manufacture of joints.

Table 9: Welding parameters

Parâmetros	Valores
Controlo FSW	Força Vertical
Direção de Rotação	CW
Velocidade de Penetração	0,1 mm/s
Dwell Time	6 s
Ângulo de Inclinação	0°
Velocidade de avanço	70 mm/min
Velocidade de rotação	1000 rpm
Força axial	450 kgf
Comprimento do pino	3,5 mm

SUBTITLE: Parameters / Values   tilt angle
FSW Control   forward speed
direction of rotation   Rotation speed
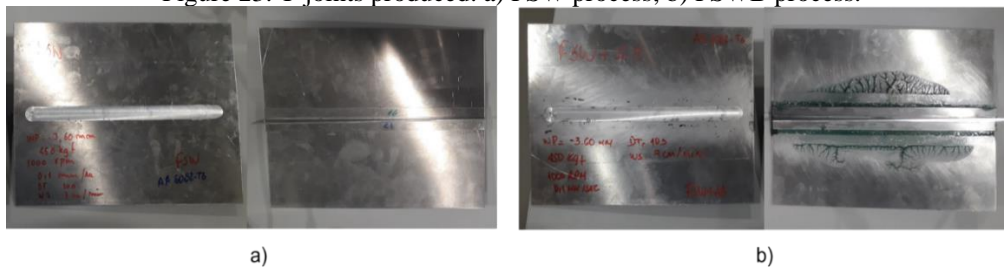penetration speed   axial force
dry time   pin length

Figure 23 shows the T-joints produced by the FSW and FSWB processes.

Figure 23: T-joints produced: a) FSW process; b) FSWB process.

6.5 MICROSCOPIC ANALYSIS

The microscope used for analysis was the LEICA DMS with increasing magnification values. The macroscopic images obtained for the joints manufactured FSW and FSWB are presented in Figure 24 and Figure 25 respectively.

Figure 24: FSW welding: a) General view; b) Advance side and c) Retreat side.
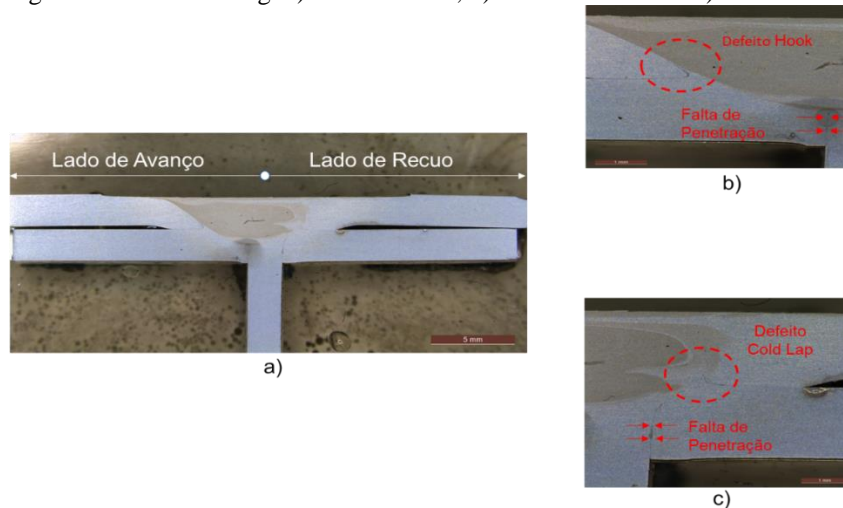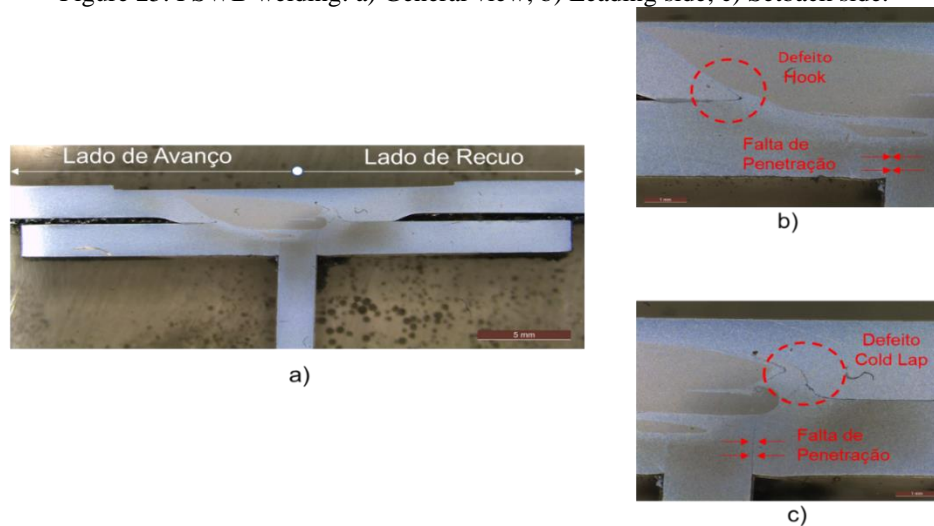
Figure 25: FSWB welding: a) General view; b) Leading side; c) Setback side.

6.6 MICROHARDNESS MEASUREMENT

The samples were also subjected to a microhardness measurement. Measurements were performed on a Digital Microhardness Tester HMV-2 (Micro Hardness Tester), applying a load of 0.2 HV (1.961 N) for 10 seconds in each indentation. The results are shown in Figure 26.

Figure 26: Microhardness values of the cross-section of the FSW sample.
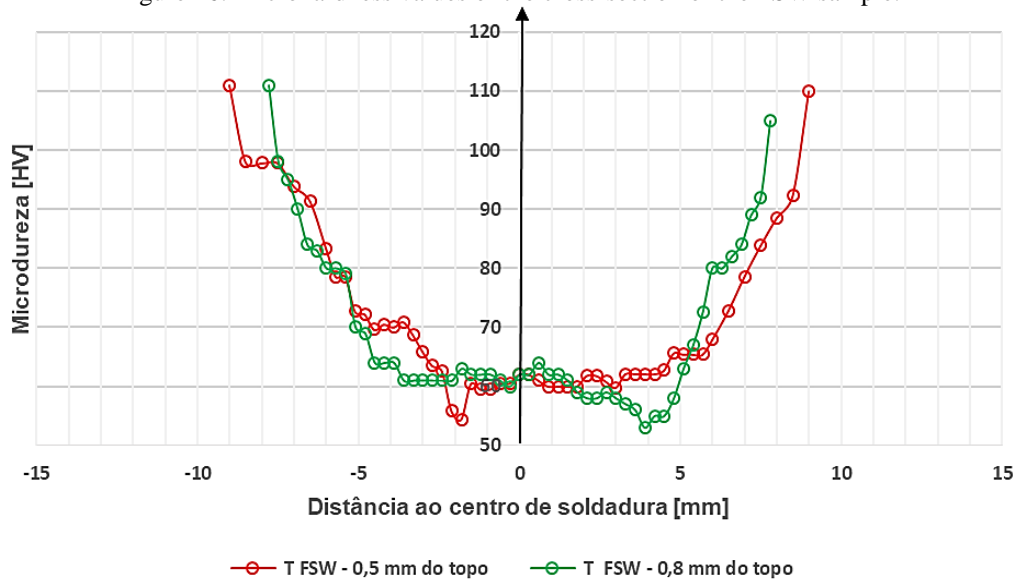
6.7 FLEXION TEST

The bending tests were carried out in accordance with the ASME standard for characterization of welding and brazing, with three points of contact, as shown in Figure 27 b). These tests were carried out on an Instron® 3369 machine with a 10 kN load cell where the punch is moved with a speed of 2 mm / min and the test was completed when the sample, Figure 26 a), was bent. During these tests, force and displacement were recorded.

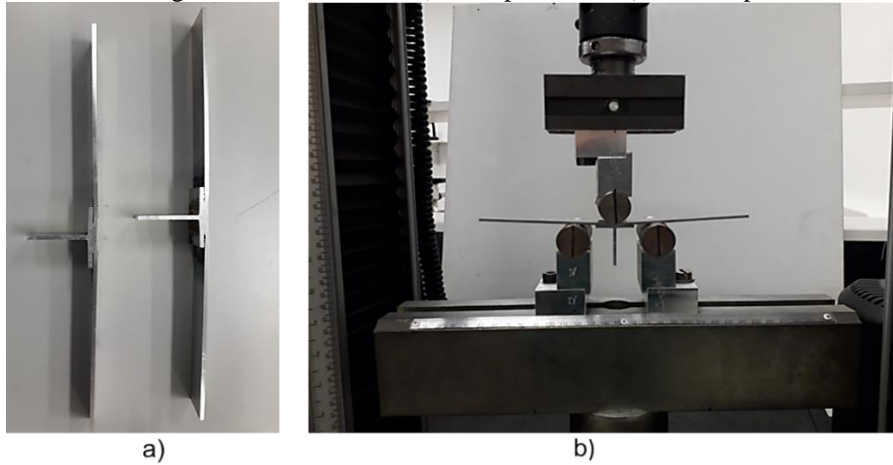Figure 27: Flexion Test: a) Test specimens; b) Test setup.

Table 10 lists all FSW and FSWB T-joints produced and the parameter combinations used in this study.

Table 10: T-joints produced

Board designation	Pin Length [mm]	Axial Force [kgf]	Rotation Speed [rpm]	Advance Speed [mm/min]
FSWB 1	3,5	450	1250	100
FSWB 2	3,5	475	1250	100
FSW 1	3,7	450	1000	70
FSWB 3	3,9	450	1000	70
FSW 2	3,9	450	1000	70
FSWB 4	4,0	450	1250	70
FSWB 5	4,0	450	1000	100
FSWB 6	4,0	475	1000	130
FSWB 7	4,2	450	1000	100
FSWB 8	4,2	475	1250	130
FSWB 9	4,4	450	1250	100

The data recorded in these tests of the FSWB joints are shown in Figure 28.

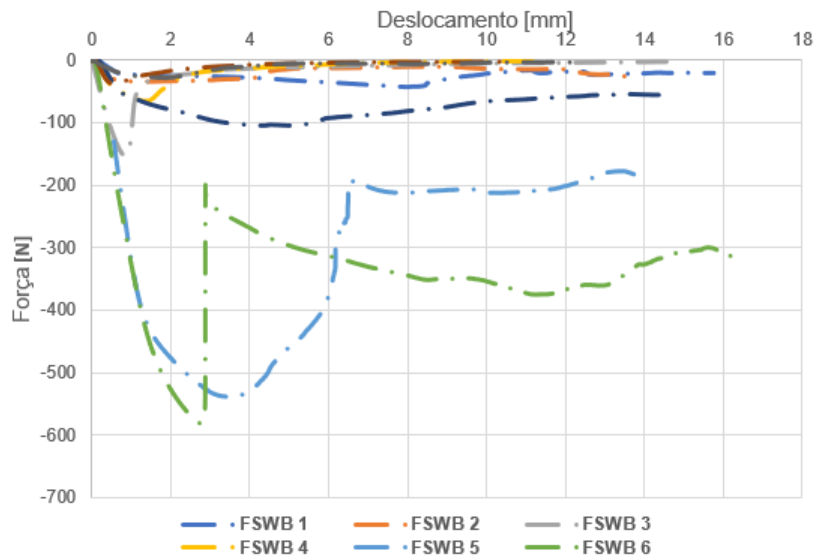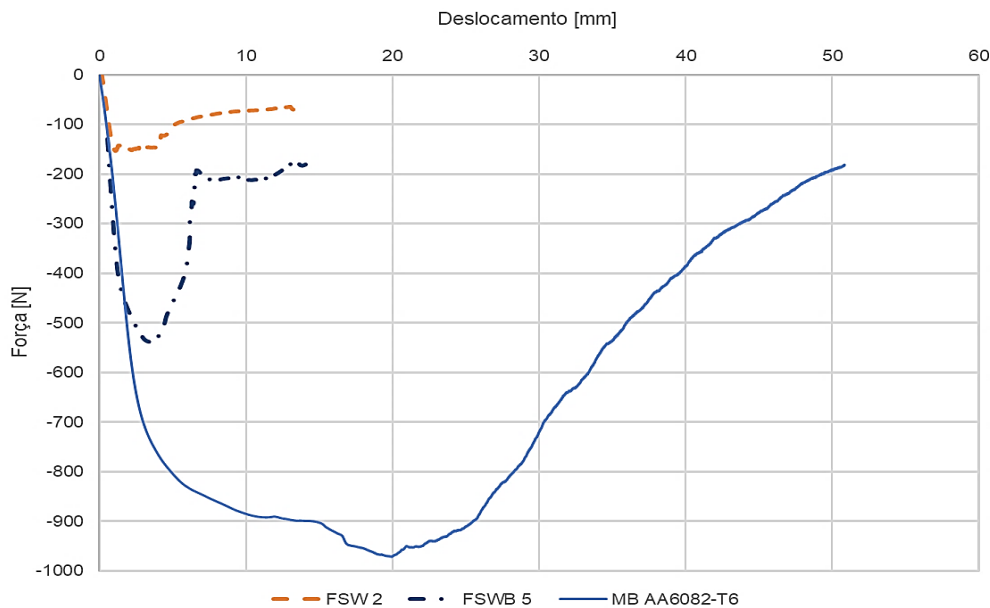Figure 28: Flexion test of FSWB joints.

Figure 29 shows the data recorded in the bending test for the base material AA6082-T6 and for the T-joints, FSW 2 and FSWB 5.

7 FINAL CONSIDERATIONS

The main objective of this article was the successful fabrication of lap and T-joints by the Friction Stir Weld-Bonding (FSWB) process. I The development of this new bonding technology, combining FSW with adhesive application (AB), resulting in bonding by hybrid welding, were compared with FSW and adhesive joints, regarding their quasi-static and fatigue performance. Below are the main conclusions of this investigation:

- The FSWB process revealed better efficiency and greater fatigue strength when compared to the FSW process.
- In quasi-static testing, FSWB lap joints showed greater strength and ductility than FSW joints. When comparing the rupture stress of the joints produced with the base material, the average efficiency of the FSWB joint was 73.75%, however, in one of the samples, it reached a value of 85.21%.
- In cyclic loading, the adhesive bond achieved the highest fatigue strength followed by FSWB welding and FSW which showed significantly lower fatigue strength (41.6% strength of adhesive joints in 106 cycles).
- T-joints, with four components, were successfully manufactured in the FSW and FSWB processes. The joints manufactured by the FSWB process obtained better results than the joints produced by FSW, but with a lower mechanical performance than the base material.

REFERENCES

[1] European Commission (2009) 'Directive 2009/33/EC - Clean and energy-efficient road transport vehicles', (June 2006), pp. 5–12. Available at: https://eur-lex.europa.eu/legal-content/EN/TXT/PDF/?uri=CELEX:32009L0033&from=EN.

[2] Peeters, P. M., J., M. and A., H. (2005) 'Fuel efficiency of commercial aircraft NLR-CR-2005-669', (November), pp. 1–37. Available at: http://www.transportenvironment.org/sites/te/files/media/2005-12_nlr_aviation_fuel_efficiency.pdf.

[3] Reynolds, C. and Kandlikar, M. (2007) 'How hybrid-electric vehicles are different from conventional vehicles: The effect of weight and power on fuel consumption', Environmental Research Letters, 2(1). doi: 10.1088/1748-9326/2/1/014003.

[4] Maciel RL, Infante V, Braga D, Moreira P, Bento T, da Silva L. Development of hybrid friction stir welding and adhesive bonding single lap joints in aluminium alloys. Fratt Integr Strutt. 2019;13(48):269-285.

[5] Prabhukhot, A. R., (2015) 'Effect of Heat Treatment on Hardness and Corrosion Behavior of 6082-T6 Aluminium Alloy in Artificial Sea Water', International Journal of Materials Science and Engineering, 3(4), pp. 286-294.

[6] Mazza, J. and Storage, K. (2011) 'Evaluation of Adhesive Bond Primers for Repair Bonding of Aluminum', 7th Bi-Annual DOD JOCOTAS Meeting with Rigid & Soft Wall Shelter Industry & Indoor & Outdoor, pp.1-48.

[7] Huntsmann Advanced Materials, (2004), 'Araldite® 420 A/B Two components epoxy adhesive', Publication No. A 161 g GB, Cambridge, England.

[8] R. Maciel, D. Braga, T. Bento, V. Infante, P. Moreira, L. da Silva "Fatigue properties of combined friction stir and adhesively bonded AA6082-T6 overlap joints" Fatigue Fract Eng Mater Struct; 1-12, 2020. https://doi.org/10.1111/ffe.13287

[9] Budynas, R. G. and Nubett, J. K. (2011) 'Elementos de Máquina de Shigley-Projeto de Engenharia Mecânica', Oitava edição, Mc Graw Hill – AMGH Editora Ltda, Porto Alegre, Brasil

[10] Mazza, J. and Storage, K. (2011) 'Evaluation of Adhesive Bond Primers for Repair Bonding of Aluminum', 7th Bi-Annual DOD JOCOTAS Meeting with Rigid & Soft Wall Shelter Industry & Indoor & Outdoor, pp.1-48.

[11] Palm, F. (2008) 'Can welding be an option in future fuselage structures – Lessons learnt and new concepts derived from 10 years in laser beam welding research', TWI-EWI seminar on Joining of Aerospace Materials, Tolouse, France.

[12] Darwish, S. M. H. (2011) 'Science of Weld: Adhesive Joints', Springer Berlin Heidelberg, Germany.

[13] ASTM D1002, (2005) 'Standard Test Method for Apparent Shear Strength of Single-Lap-Joint Adhesively Bonded Metal Specimens by Tension Loading (Metal-to-Metal)', Annual Book of ASTM Standards, 15.06.

[14] Bahemmat, P., Besharati, M. K., Haghpanahi, M., Rahbari, A. and Salekrostam, R. (2009) 'Mechanical, micro, and macrostructural analysis of AA7075–T6 fabricated by friction stir butt welding with different rotational speeds and tool pin profiles'. J. Engineering Manufacture, 224 Part B, pp. 419-433. doi: 10.1243/09544054JEM1554.

[15] Reynolds, A. P. (1999) 'Visualisation of material flow in autogeneous friction stir welds'. Science and technology of welding and joining, 5, pp. 120-125.

[16] Misha, R. S. and Ma, Z. Y. (2005) 'Friction stir welding and processing'. Materials Science and Engineering, R 50, pp. 1-78. doi: 10.1016/j.mser 2005.07.001.

[17] Infante, V. et al. (2015) 'Study of the fatigue behaviour of dissimilar aluminium joints produced by friction stir welding', International Journal of Fatigue, Elsevier Ltd. doi: 10.1016/j.ijfatigue.2015.06.020.

[18] Buffa, G. et al. (2008) 'Material Flow in FSW of T-joints: Experimental and Numerical Analysis', 1, pp.1283-1286. doi: 10.1007/s12289-0137-6.

[19] Ram, G. D. J. et al. (2012) 'Microstructure and Mechanical Properties of Friction Stir Lap Welded Aluminum Alloy AA2014', Journal of Materials Science & Technology. The Chinese Society for Metals, 28(5), pp. 414–426. doi: 10.1016/S1005-0302(12)60077-2.

[20] Castillo, E. and Canteli, A. F. (2009) 'A Unified Statistical Methodology for Modeling Fatigue Damage', Springer Science and Business Media B.V., doi: 10.1007/978-1-4020-9182-7.

[21] Braga, D. F. O. et al. (2018) 'Fatigue performance of hybrid overlap friction stir welding and adhesive bonding of an Al - Mg - Cu alloy', Fatigue Fract Eng Mater Struct, pp. 1–9. doi: 10.1111/ffe.12933.

[22] Fratini, L. et al. (2009) 'Experimental Characterization of FSW T-Joints of Light Alloys', Key Engineering Materials, 344, pp. 751–758. doi: 10.4028/www.scientific.net/kem.344.751.

[23] Fratini, L. and Gagliardi, F. (2006) 'Friction Stir Welding of AA6082-T6 T-joints : process engineering and performance measurement', J. Engineering Manufacture – Imeche, 220 – part B, pp. 669-676. doi: 10.1243/09544054JEM327.